

The Computation of the Magnetic Field of any Axisymmetric Current Distribution—with Magnetospheric Applications

P. C. Kendall,* S. Chapman,† S.-I. Akasofu‡ and P. N. Swartztrauber §

(Received 1965 August 5)

Summary

It is shown that the vector potential \mathbf{A} of the magnetic field of any axisymmetric electric current distribution can be expressed in the form $\Sigma A_n(r)P_n^1(\cos \theta)$. This series is used to compute the field of two model magnetospheric ring currents; the field of one of these was previously determined by double integrations by Akasofu, Cain & Chapman. The calculation of the functions $A_n(r)$ does not require double integrations. The two sets of results are in good agreement. The first term in the series for \mathbf{A} gives the external magnetic moment of the ring current. The magnetic field energy is calculated for the field as a whole and for each term in the series for \mathbf{A} . The field isointensity lines are drawn, and also the field lines for the ring current and for its field combined with that of the geomagnetic dipole. They illustrate the considerable distortion of the field in the magnetosphere during magnetic storms. The series for \mathbf{A} may also be helpful in calculating the paths of cosmic rays in the deformed magnetosphere.

The numerical convergence of the results is improved by the use of Cesàro summation.

1. Introduction

Gauss (1838) was the pioneer in the application of spherical harmonic functions to the analytic expression of the geomagnetic field. Later Schuster (1889) extended their application to the changing field of the daily magnetic variations. These are attributed to electric currents that flow mainly in a rather thin layer of the ionosphere. Such currents and their field can usefully be discussed in terms of a model surface current flow at a constant height above the ground; the scalar potential of its magnetic field outside and within the surface can be expressed very simply

* Geophysical Institute, College, Alaska (Permanent address: Department of Applied Mathematics, The University, Sheffield 10).

† Geophysical Institute, College, Alaska; High Altitude Observatory, Boulder, Colorado; and Institute of Science and Technology, University of Michigan, Ann Arbor, Michigan.

‡ Geophysical Institute, College, Alaska.

§ National Center for Atmospheric Research, Boulder, Colorado.

in terms of the spherical harmonic expression for the surface current function (Chapman & Bartels 1940, pp. 630, 631). This method is less convenient in connection with volume current distributions, although such distributions can be treated as combinations of spherical shells. For volume distributions it is best to express the magnetic field in terms of the vector potential \mathbf{A} , which unlike the scalar potential exists everywhere. We show that \mathbf{A} can be expressed in the form of a series $\sum A_n(r)P_n^1(\cos \theta)$. This is used to calculate the fields of two ring current systems previously considered by Akasofu & Chapman (1961) and Akasofu, Cain & Chapman (1961, 1962). They determined the fields by double integrations over the cross section of the current. The method here given does not involve such integrations, and gives the field more simply and generally, at any point.

The results of the two sets of calculations are compared and found to agree well. The field lines of the ring current are drawn, alone and also in combination with the geomagnetic dipole field. The magnetic field energy is calculated for the whole ring current field, and for each term in the series for \mathbf{A} . The external magnetic moment of the ring current is found. The results are of interest in connection with magnetic storms.

The convergence of the numerical results is improved by the use of Cesàro summation.

2. The vector potential \mathbf{A} of an axisymmetric electric current distribution $\mathbf{j}(r, \theta)$

In considering axisymmetric current distributions and their magnetic fields, spherical polar coordinates r, θ, Φ for any point P are appropriate; $\mathbf{e}_r, \mathbf{e}_\theta, \mathbf{e}_\Phi$ will denote a right-handed orthogonal triad of unit vectors along the respective directions of increasing r, θ, Φ at P . The current intensity \mathbf{J} is given by

$$\mathbf{J} = J(r, \theta)\mathbf{e}_\Phi. \quad (1)$$

We shall suppose that the current distribution lies between the spherical surfaces $r = r_1$ and $r = r_2 (> r_1)$. The vector potential \mathbf{A} is likewise given by

$$\mathbf{A} = A(r, \theta)\mathbf{e}_\Phi. \quad (2)$$

By using the known formula for the vector potential of a circular line current (Smythe 1950, p. 271) it is clearly possible to express $A(r, \theta)$ in the form of a double integral over the axial cross section S . In mixed Gaussian units (c = velocity of light) this integral is

$$A(r, \theta) = \frac{2}{cr \sin \theta} \iint_S G(r, \theta; r_0, \theta_0) J(r_0, \theta_0) r_0 \, dr_0 \, d\theta_0, \quad (3)$$

where

$$G = L[(1 - \frac{1}{2}k^2)K(k) - E(k)], \quad (4)$$

$$L^2 = r^2 + r_0^2 - 2rr_0 \cos(\theta + \theta_0), \quad (5)$$

$$k^2 = 4rr_0 \sin \theta \sin \theta_0 / L^2 \quad (6)$$

and K and E are elliptic integrals of the first and second kinds. From (3) it is possible to derive expressions for the radial and θ components of the magnetic intensity \mathbf{h} (= curl \mathbf{A}) of the field of the current distribution, each in the form of a double integral. Such expressions have been given by Akasofu & Chapman (1961, their equations 76, 77).

Here, however, we express \mathbf{A} in terms of spherical functions. When \mathbf{A} has the form (2), Ampère's equation

$$\text{curl curl } \mathbf{A} = 4\pi\mathbf{J}/c$$

is equivalent to

$$\frac{\Delta(Ar \sin \theta)}{r \sin \theta} = \frac{4\pi J(r, \theta)}{c}, \tag{7}$$

where Δ denotes the differential operator given by

$$\Delta \equiv \frac{\partial^2}{\partial r^2} + \frac{(1-\mu^2)}{r^2} \frac{\partial^2}{\partial \mu^2}, \quad \mu = \cos \theta. \tag{8}$$

Hence it is convenient to write

$$A(r, \theta)r \sin \theta = \psi(r, \theta). \tag{9}$$

In terms of ψ the magnetic intensity \mathbf{h} is given by

$$\mathbf{h} = h_r \mathbf{e}_r + h_\theta \mathbf{e}_\theta, \quad h_r = \frac{1}{r^2 \sin \theta} \frac{\partial \psi}{\partial \theta}, \quad h_\theta = -\frac{1}{r \sin \theta} \frac{\partial \psi}{\partial r}. \tag{10}$$

Consequently the \mathbf{h} field lines are given by

$$h_\theta dr - h_r r d\theta = 0 \quad \text{or} \quad d\psi = 0 \quad \text{or} \quad \psi = \text{constant}. \tag{11}$$

Thus the function ψ may be called the magnetic stream function, by analogy with the Stokes stream function in fluid flow.

In terms of ψ , (7) has the form

$$\Delta\psi = \frac{\partial^2 \psi}{\partial r^2} + \frac{(1-\mu^2)}{r^2} \frac{\partial^2 \psi}{\partial \mu^2} = \frac{4\pi r \sin \theta}{c} J(r, \theta). \tag{12}$$

We express ψ as a sum of terms each of which is a product $A_n(r)p_n(\mu)$; this term will contribute to $\Delta\psi$ as follows:

$$\frac{A_n p_n}{r^2} \left[\frac{r^2}{A_n(r)} \frac{d^2 A_n}{dr^2} + \frac{(1-\mu^2)}{p_n(\mu)} \frac{d^2 p_n}{d\mu^2} \right]. \tag{13}$$

In the regions within the sphere $r = r_1$ and outside the sphere $r = r_2$, where $J = 0$ and $\Delta\psi = 0$, A_n and p_n are chosen so that (13) is zero for every value of n ; (13) is zero if the two terms in the bracket are numerically equal constants, of opposite sign. In order that $p_n(\mu)$ may be non-singular at $\mu = \pm 1$ the constant must be of the form $n(n+1)$, where n is a positive integer. Then $A_n(r)$ is a constant multiple of either r^{n+1} or r^{-n} ; the former is appropriate in the region $r < r_1$, the other applies to the region $r > r_2$. Then the associated function p_n satisfies the equation

$$(1-\mu^2) \frac{d^2 p_n(\mu)}{d\mu^2} + n(n+1)p_n(\mu) = 0. \tag{14}$$

The appropriate solution of this equation is

$$p_n(\mu) = (1-\mu^2) \frac{dP_n(\mu)}{d\mu} = P_n^1(\mu) \sin \theta. \tag{15}$$

Here P_n denotes the Legendre function, and P_n^1 the associated Legendre function of degree n and order unity [$P_n^1(\mu) = \sin \theta dP_n(\mu)/d\mu$].

Thus for the two regions within $r = r_1$ and outside $r = r_2$ the series for ψ have the following form :

$$(r < r_1) \quad \psi = \sum_{n=1}^{\infty} i_n r^{n+1} P_n^1(\mu) \sin \theta, \quad (r > r_2) \quad \psi = \sum_{n=1}^{\infty} e_n r^{-n} P_n^1(\mu) \sin \theta. \quad (16)$$

For points between the two surfaces $r = r_1$ and $r = r_2$, the functions $A_n(r)$ in the series expression

$$\psi = \sum_{n=1}^{\infty} A_n(r) P_n(\mu), \quad (17)$$

where $p_n(\mu)$ is taken to have the form (15), must each satisfy the equation

$$\frac{d^2 A_n(r)}{dr^2} - \frac{n(n+1)}{r^2} A_n(r) = j_n(r). \quad (18)$$

Here $j_n(r)$ denotes the factor shown in the following expression for part of the term on the right hand side of (12),

$$(4\pi r/c) J(r, \theta) = \sum_{n=1}^{\infty} j_n(r) P_n^1(\mu). \quad (19)$$

Hence

$$j_n(r) = \frac{2n+1}{2n(n+1)} \frac{4\pi r}{c} \int_{-1}^1 J(r, \theta) P_n^1(\mu) d\mu. \quad (20)$$

The solutions of (18) each contain two arbitrary constants; these are determined by making $A_n(r)$ satisfy the two boundary conditions

$$dA_n(r)/dr = (n+1)A_n(r)/r \text{ at } r = r_1, \quad dA_n(r)/dr = -nA_n(r)/r \text{ at } r = r_2. \quad (21)$$

The magnetic potential inside the sphere $r = r_1$ will then be harmonic, and finite at the origin. The magnetic potential outside the sphere $r = r_2$ will also be harmonic, and approach zero as $r \rightarrow \infty$. The values of $A_n(r)$ thus found at $r = r_1$ and $r = r_2$ give the values of i_n and e_n in (16).

By (10, 17) the magnetic intensity \mathbf{h} of the current distribution is given by

$$h_r = \sum_{n=1}^{\infty} n(n+1)A_n(r)P_n(\mu)/r^2, \quad h_\theta = - \sum_{n=1}^{\infty} (dA_n/dr)P_n^1(\mu)/r. \quad (22)$$

3. Model current systems

Suitably scaled multiples $a_n(r/a)$ (Section 4) of the functions $A_n(r)$ (Section 2) have been determined numerically for two model electric current distributions (Akasofu & Chapman 1961) of the form (1), using (18, 20, 21). The method of computation is described in Section 4. Each distribution relates to a set of particles of maximum number density n , all having the same translatory kinetic energy E , moving in the field \mathbf{H} of the Earth magnetic dipole, of moment M . Both models are versions of the distribution

$$J(r, \theta) = (2ca^2 n_0 E/M) j(k, \theta), \quad (23)$$

where

$$k = (r/a) \operatorname{cosec}^2 \theta, \quad (24)$$

and a denotes the radius of the Earth; $j(k, \theta)$ is given as follows:

$$\text{for } k \leq k_0, \quad j(k, \theta) = -\{f_1(\alpha, \theta) - 2g_1^2(k - k_0)f_2(\alpha, \theta)\} \exp\{-g_1^2(k - k_0)^2\}; \quad (25)$$

$$\text{for } k \geq k_0, \quad j(k, \theta) = -\{f_1(\alpha, \theta) - 2g_2^2(k - k_0)f_2(\alpha, \theta)\} \exp\{-g_2^2(k - k_0)^2\}, \quad (26)$$

where

$$f_1(\alpha, \theta) = \frac{3k^2\alpha(\sin \theta)^{5+3\alpha}(1 + \cos^2 \theta)}{2(\alpha + 3)(1 + 3 \cos^2 \theta)^{2+\alpha/4}} \quad (27)$$

and

$$f_2(\alpha, \theta) = \frac{k^3(\alpha + 2)(\sin \theta)^{3+3\alpha}}{2(\alpha + 3)(1 + 3 \cos^2 \theta)^{\alpha/4}}. \quad (28)$$

For both models r_1 is taken to be a , and r_2 is taken to be $10a$; but $n(r, \theta)$ and $j(r, \theta)$ are so small beyond these limits that an extension of them inward and outward would add inappreciably to the current distribution and its field.

In the outer part of the belt the current is westward, and in the inner part it is eastward. The field of the currents is supposed to be negligibly weak compared with the total field.

As the distribution $j(r, \theta)$ is symmetrical about the equatorial plane $\theta = 90^\circ$, all the functions A_n for even values of n are zero. We have computed suitable multiples of A_n (Section 4) for the eleven odd values of n from 1 to 21, for two sets of the numerical constants α, k_0, g_1, g_2 involved in the distribution given by (23–28), and for values of $R (= r/a)$ from 1 to 10 at intervals of 0.01. The values of $a_n(R)$ and of $da_n(R)/dR$, in each case, are given in Table 1 for $n = 1, 3, 5$ at intervals of $0.2r/a$ (see Section 4); the results for the other values of n and r/a are stored on magnetic tape, and are available to suitable users by arrangement with P. C. Kendall.

The two sets of constants of the distributions are as follows:

I. $\alpha = -\frac{1}{2}, k_0 = 6, g_1 = g_2 = (\ln 10)^{\frac{1}{2}} = 1.517$ (to four significant figures), (Akasofu & Chapman 1961).

II. $\alpha = 2, k_0 = 3, g_1 = 2.990, g_2 = 0.419$ (Akasofu 1963).

Thus in the first case,

$$e^{-g^2(k-k_0)^2} = 0.1 \quad \text{for } k - k_0 = \pm 1.$$

The current distribution given by (23–28) is that of a certain density distribution $n(r, \theta)$ of charged particles all of the same mass m , charge e and speed v moving with a certain pitch angle distribution $f(\phi)$ of velocities \mathbf{v} in the field of the Earth dipole, whose axis is taken as the polar axis of the coordinates r, θ, Φ . Here ϕ denotes the angle between \mathbf{v} and \mathbf{H}_e , the value of \mathbf{H} at the point considered; this angle is called the pitch angle. The definition of $f(\phi)$ is the statement that $f(\phi) d\phi$ is the fraction of particles at r_e that have pitch angles between ϕ and $\phi + d\phi$.

The chosen model distributions $f(\phi)$ and $n(r, \theta)$ at a point P_e in the dipole equatorial plane, at distance r_e from the origin (at the Earth's centre) are given by

$$f(\phi) = C_\alpha \sin^{\alpha+1} \phi \quad (29)$$

and

$$n(r_e) = n_0 e^{-(g_1 z_e)^2} \quad \text{for } r_e < k_0 a, \quad n(r_e) = n_0 e^{-(g_2 z_e)^2} \quad \text{for } r_e > k_0 a. \quad (30)$$

In (30),

$$z_e = (r_e/a) - k_0. \quad (31)$$

Table 1
The spatial variations of $a_n(R)$ and $da_n(R)/dR$ for $n = 1, 3, 5$; models I and II.
 Entries r_s in the table should be interpreted as $r \times 10^8$

n R	Model I					Model II					
	$a_n(R)$	$da_n(R)/dR$	$a_n(R)$	$da_n(R)/dR$	$a_n(R)$	$da_n(R)/dR$	$a_n(R)$	$da_n(R)/dR$	$a_n(R)$	$da_n(R)/dR$	
1-0	-1.218+1	-1.354-2	-4.065-3	-2.436+1	-5.414-2	-2.439-2	-5.141+0	-1.056-2	-1.028+1	-4.225-2	4.781-3
1-2	-1.754+1	-2.810-2	-1.100-2	-2.921+1	-9.373-2	-4.686-2	-7.403+0	-2.206-2	-1.234+1	-7.495-2	1.212-2
1-4	-2.387+1	-5.196-2	-2.351-2	-3.413+1	-1.473-1	-7.974-2	-1.008+1	-4.162-2	-1.440+1	-1.239-1	2.881-2
1-6	-3.118+1	-8.794-2	-4.335-2	-3.896+1	-2.148-1	-1.192-1	-1.316+1	-7.310-2	-1.648+1	-1.954-1	6.686-2
1-8	-3.946+1	-1.387-1	-7.112-2	-4.390+1	-2.945-1	-1.573-1	-1.667+1	-1.217-1	-1.859+1	-2.961-1	1.519-1
2-0	-4.873+1	-2.063-1	-1.053-1	-4.875+1	-3.823-1	-1.807-1	-2.061+1	-1.934-1	-2.080+1	-4.232-1	3.289-1
2-2	-5.897+1	-2.917-1	-1.411-1	-5.368+1	-4.710-1	-1.698-1	-2.501+1	-2.897-1	-2.326+1	-5.261-1	6.469-1
2-4	-7.021+1	-3.940-1	-1.693-1	-5.865+1	-5.497-1	-9.938-2	-2.996+1	-3.875-1	-2.642+1	-3.692-1	1.039+0
2-6	-8.242+1	-5.098-1	-1.749-1	-6.351+1	-6.025-1	6.120-2	-3.569+1	-3.786-1	-3.122+1	6.694-1	1.047+0
2-8	-9.563+1	-6.319-1	-1.365-1	-6.861+1	-6.075-1	3.463-1	-4.257+1	-3.693-2	-3.765+1	2.857+0	2.229-1
3-0	-1.099+2	-7.477-1	-2.568-2	-7.356+1	-5.353-1	7.914-1	-5.063+1	7.221-1	-4.238+1	4.456+0	-3.295-1
3-2	-1.251+2	-8.383-1	-1.929-1	-7.869+1	-3.470-1	1.429+0	-5.941+1	1.703+0	-4.544+1	5.387+0	-4.129-1
3-4	-1.413+2	-8.754-1	-5.604-1	-8.392+1	8.490-3	2.283+0	-6.879+1	2.887+0	-4.827+1	6.473+0	-6.430-1
3-6	-1.586+2	-8.193-1	1.121+0	-8.917+1	5.986-1	3.361+0	-7.870+1	4.298+0	-5.071+1	7.636+0	-9.923-1
3-8	-1.770+2	-6.145-1	1.919+0	-9.470+1	1.512+0	4.641+0	-8.904+1	5.941+0	-5.259+1	8.791+0	-1.431+0
4-0	-1.965+2	-1.847-1	2.987+0	-1.004+2	2.872+0	6.055+0	-9.968+1	7.808+0	-5.375+1	9.849+0	-1.923+0
4-2	-2.172+2	5.751-1	4.340+0	-1.065+2	4.848+0	7.458+0	-1.105+2	9.869+0	-5.406+1	1.072+1	-2.427+0
4-4	-2.392+2	1.813+0	5.952+0	-1.133+2	7.700+0	8.581+0	-1.212+2	1.208+1	-5.341+1	1.134+1	-2.900+0
4-6	-2.626+2	3.740+0	7.723+0	-1.211+2	1.183+1	8.953+0	-1.318+2	1.438+1	-5.177+1	1.164+1	-3.301+0
4-8	-2.877+2	6.669+0	9.433+0	-1.305+2	1.783+1	7.810+0	-1.419+2	1.671+1	-4.915+1	1.159+1	-3.592+0
5-0	-3.150+2	1.105+1	1.068+1	-1.423+2	2.643+1	4.108+0	-1.514+2	1.899+1	-4.561+1	1.117+1	-3.745+0
5-2	-3.448+2	1.744+1	1.084+1	-1.564+2	3.799+1	-3.122+0	-1.601+2	2.116+1	-4.125+1	1.039+1	-3.745+0

Table 1—continued

54	-3-776+2	2-638+1	9-187+0	-1-707+2	5-151+1	-1-388+1	-1-678+2	2-313+1	-4-742+0	-3-625+1	9-297+0	-3-588+0
56	-4-127+2	3-796+1	5-181+0	-1-791+2	6-367+1	-2-613+1	-1-745+2	2-486+1	-5-432+0	-5-078+1	7-943+0	-3-284+0
58	-4-482+2	5-140+1	-1-089+0	-1-732+2	6-917+1	-3-572+1	-1-801+2	2-629+1	-6-047+0	-2-504+1	6-399+0	-2-853+0
60	-4-806+2	6-487+1	-8-628+0	-1-467+2	6-347+1	-3-823+1	-1-846+2	2-741+1	-6-566+0	-1-924+1	4-741+0	-2-323+0
62	-5-056+2	7-601+1	-1-579+1	-1-012+2	4-627+1	-3-201+1	-1-878+2	2-819+1	-6-972+0	-1-356+1	3-048+0	-1-730+0
64	-5-205+2	8-295+1	-2-102+1	-4-719+1	2-260+1	-1-962+1	-1-900+2	2-863+1	-7-256+0	-8-173+0	1-393+0	-1-108+0
66	-5-249+2	8-512+1	-2-357+1	1-816+0	-9-960-2	-6-130+0	-1-911+2	2-875+1	-7-415+0	-3-202+0	-1-606-1	-4-903-1
68	-5-207+2	8-335+1	-2-369+1	3-656+1	-1-634+1	4-173+0	-1-913+2	2-858+1	-7-455+0	1-250+0	-1-563+0	9-211-2
70	-5-113+2	7-911+1	-2-222+1	5-561+1	-2-481+1	9-788+0	-1-907+2	2-814+1	-7-383+0	5-125+0	-2-779+0	6-161-1
72	-4-993+2	7-382+1	-2-003+1	6-295+1	-2-737+1	1-159+1	-1-893+2	2-748+1	-7-213+0	8-397+0	-3-790+0	1-065+0
74	-4-865+2	6-838+1	-1-772+1	6-378+1	-2-666+1	1-124+1	-1-874+2	2-664+1	-6-962+0	1-107+1	-4-588+0	1-430+0
76	-4-740+2	6-323+1	-1-559+1	6-185+1	-2-469+1	1-006+1	-1-849+2	2-566+1	-6-647+0	1-317+1	-5-181+0	1-707+0
78	-4-618+2	5-852+1	-1-371+1	5-910+1	-2-245+1	8-744+0	-1-821+2	2-458+1	-6-285+0	1-476+1	-5-583+0	1-900+0
80	-4-503+2	5-425+1	-1-208+1	5-627+1	-2-033+1	7-543+0	-1-790+2	2-344+1	-5-892+0	1-588+1	-5-815+0	2-015+0
82	-4-393+2	5-037+1	-1-068+1	5-357+1	-1-843+1	6-510+0	-1-758+2	2-226+1	-5-483+0	1-661+1	-5-903+0	2-063+0
84	-4-289+2	4-686+1	-9-467+0	5-106+1	-1-674+1	5-635+0	-1-724+2	2-108+1	-5-071+0	1-701+1	-5-873+0	2-056+0
86	-4-189+2	4-367+1	-8-416+0	4-871+1	-1-523+1	4-893+0	-1-690+2	1-992+1	-4-664+0	1-714+1	-5-750+0	2-004+0
88	-4-094+2	4-076+1	-7-502+0	4-652+1	-1-389+1	4-263+0	-1-656+2	1-879+1	-4-271+0	1-707+1	-5-560+0	1-919+0
90	-4-003+2	3-810+1	-6-705+0	4-448+1	-1-270+1	3-725+0	-1-622+2	1-770+1	-3-898+0	1-684+1	-5-322+0	1-812+0
92	-3-916+2	3-567+1	-6-007+0	4-256+1	-1-163+1	3-265+0	-1-589+2	1-666+1	-3-547+0	1-651+1	-5-054+0	1-692+0
94	-3-832+2	3-344+1	-5-395+0	4-077+1	-1-067+1	2-869+0	-1-556+2	1-568+1	-3-221+0	1-609+1	-4-770+0	1-566+0
96	-3-753+2	3-139+1	-4-856+0	3-909+1	-9-810+0	2-529+0	-1-524+2	1-478+1	-2-921+0	1-563+1	-4-483+0	1-439+0
98	-3-676+2	2-951+1	-4-380+0	3-751+1	-9-034+0	2-235+0	-1-493+2	1-388+1	-2-645+0	1-514+1	-4-199+0	1-316+0
100	-3-603+2	2-777+1	-3-959+0	3-603+1	-8-332+0	1-980+0	-1-464+2	1-307+1	-2-394+0	1-464+1	-3-924+0	1-199+0

The v distribution is supposed to be symmetrical about an axis along the field intensity H_e at P_e , and is concerned only with the distribution of ϕ because the speeds v are taken to be all alike. The distribution (29) is specially simple and mathematically advantageous because, as Parker (1957) showed, if valid at one point along a field line (in a general field, not only in a dipole field) it is valid all along the line; α might differ from line to line, but here it is taken to have the same value for all field lines (or all values of r_e). Moreover, Parker (1957) showed (for a general field) that with this velocity distribution, for particles of a given speed, $n(r, \theta)$ at other points along the same field line is related to its value at the point where $H = H_e$ by the relation.

$$n(r, \theta) = n(r_e)(H_e/H)^{\alpha/2}. \quad (32)$$

For the dipole field, H at the point with polar angle θ , on the field line that crosses the dipole equatorial plane at r_e , is given by

$$H_e/H = \sin^6\theta/(1 + 3 \cos^2\theta). \quad (33)$$

Equations (29–33) fully specify the model belts here considered. The above definition of $f(\phi)$ implies that

$$\int_0^\pi f(\phi) d\phi = 1;$$

this condition determines the value of C_α , namely

$$C_\alpha = \frac{\Gamma(\alpha+2)}{2^{\alpha+1}\{\Gamma(\frac{1}{2}\alpha+1)\}^2}, \quad (34)$$

where $\Gamma(x)$ denotes the complete gamma function with argument x .

Clearly the density distribution (30) in the equatorial plane is Gaussian and symmetric in model I, and Gaussian with different spreads on each side of $r_e = k_0a$ in model II. In each model the maximum density is n_0 ; in model I the density sinks to $n_0/10$ at a distance of one Earth radius on either side of the point of maximum density. Model II is chosen to agree with a certain observed density distribution, so that the parameters g have no simple expression as in the case of model I. From the equatorial plane the belt of particles bends downwards to north and south towards the Earth, approximately following the field lines. The isolines of $j(r, \theta)$ for model I have been illustrated by Akasofu & Chapman (1961, Fig. 3c, p. 1330), who also illustrate the pitch angle distribution (their Fig. 2, p. 1326); the negative value of α for model I implies an excess of small pitch angles, and conversely the positive value for model II corresponds to an excess of large pitch angles.

4. The method of computation

It is convenient to use dimensionless variables in the computations and also in formulating tables. Thus instead of r we use the variable

$$R = r/a, \quad (35)$$

and make the corresponding changes in notation

$$R_1 = r_1/a \quad R_2 = r_2/a. \quad (36)$$

Then (17) becomes

$$\psi = \mathcal{E}\psi', \quad \psi' = \sum_{n=1}^{\infty} a_n(R)P_n^1(\mu) \sin \theta, \quad (37)$$

where

$$\mathcal{E} = 8\pi a^5 n_0 E/M. \quad (38)$$

Numerically, taking $M = 0.32a^3$ Gauss cm^3 ,

$$\mathcal{E} = 1.258 \times 10^{-7} a^2 n_0 E, \quad (39)$$

where now E is measured in kev. The fundamental differential equation (18) then takes the dimensionless form

$$\frac{d^2 a_n}{dR^2} - \frac{n(n+1)a_n}{R^2} = \int_0^{\pi/2} \frac{(2n+1)}{n(n+1)} j R p_n(\mu) d\theta, \quad (40)$$

where j is given by (25) and (26). The boundary conditions (21) become

$$da_n/dR = (n+1)a_n/R \text{ at } R = R_1, \quad da_n/dR = -na_n/R \text{ at } R = R_2. \quad (41)$$

Inside the sphere $R = R_1$ and outside the sphere $R = R_2$, $a_n(R)$ has the simple forms

$$a_n(R) = c_n R^{n+1} \quad (R \leq R_1) \quad a_n(R) = d_n/R^n \quad (R \geq R_2), \quad (42)$$

where c_n and d_n are constants.

The numerical expressions for the magnetic field in Gauss are

$$h_r = 1.258 \times 10^{-7} n_0 E h'_r, \quad h'_r = \sum_{n=1}^{\infty} \frac{n(n+1)a_n(R)}{R^2} P_n(\mu), \quad (43)$$

$$h_\theta = 1.258 \times 10^{-7} n_0 E h'_\theta, \quad h'_\theta = - \sum_{n=1}^{\infty} \frac{1}{R} \frac{da_n(R)}{dR} P_n^1(\mu). \quad (44)$$

The right hand side of (40) is calculated by Simpson's rule, dividing the interval $(0, \pi/2)$ into $20n$ parts. As the functions $P_n^1(\mu)$ are oscillatory, the number of divisions must increase with n .

The vector potential coefficient functions $a_n(R)$ are then to be calculated from (40) subject to the boundary conditions (41). As (40) is linear, only a particular integral has to be determined numerically; then the boundary conditions can be satisfied by adding a suitable value of the complementary function. It is possible to find a particular integral starting with a chosen value a_{n0} at $R = R_1$, using $da_n/dR = (n+1)a_{n0}$ there, and (40); but in practice the solution rapidly becomes large and therefore inaccurate, so that effectively the boundary condition at $R = R_2$ cannot be used. Hence it was found to be necessary to adjust the solution after integrating (40) over a few step lengths. Suppose that the m th integration step from $R = R_1$ in the direction of increasing R has been reached at $R = R'_m$ (with $R'_1 = R_1$), and that all the values of the solution so far obtained ($a_{n,0}, a_{n,1}, a_{n,2}, \dots$) are stored in the computer together with the derivatives da_n/dR which arise as part of the integration process. If CR_s^{n+1} is added to $a_n(R_s)$, and $(n+1)CR_s^n$ to da_n/dR , the boundary condition (41) at $R = R_1$ is still satisfied. Therefore we choose C so that

$$da_n(R'_m)/dR + (n+1)CR_m^n = -na_n(R'_m)/R'_m - nCR_m^n, \quad (45)$$

giving

$$C = -\{da_n(R'_m)/dr + na_n(R'_m)/R'_m\}/(2n+1)R_m^n. \quad (46)$$

The modified solution then satisfies the condition of type (41) at $R = R'_m$. For a step-length 0.01, this process of modification is used at every fifth step. When $R = R_2$ is reached it is found that both boundary conditions (41) are satisfied.

The integration was advanced in stages of five steps; in the first stage the Runge-Kutta method was used (cf. Kunz 1957, p. 185). For all subsequent stages an equally accurate but faster process was used (cf. Ralston & Wilf 1960, p. 100). At the outset it was judged sufficient to calculate the first eleven functions $a_n(R)$ and their first derivatives $da_n(R)/dR$, $n = 1$ to $n = 21$. A complete computer run (taking 10 minutes on the CDC computer of the U.S. National Center for Atmospheric Research, Boulder, Colorado) gives a table of values of $a_n(R)$ and $da_n(R)/dR$ for these eleven values of n for values of R from $R_1 (= 1$ in our work) to $R_2 (= 10$ in our calculations) at intervals 0.01. The first and last values of a_n give the coefficients in (16).

The programme accuracy was checked by verifying that the magnetic intensity at the origin (the Earth's centre) found from equation (42) agreed with the value found for the same current distribution by Akasofu & Chapman (1961). The differential equation (40) was also treated by lattice methods; in this case the two solutions agreed except for the higher harmonics near $R = R_1$. As the difference between the two solutions becomes negligible even a few step-lengths away from $R = R_1$ we conclude that the difference is to be ascribed to the much lower degree of accuracy of the lattice solution; in any case, the higher harmonics contribute very little to the magnetic field \mathbf{h} near $R = R_1$. The programme was also checked by halving the step lengths for the integrations with respect to θ and r ; there was no change in the sixth decimal place even for the higher harmonics.

5. The numerical convergence of the series expressions for the field \mathbf{h}

The calculations for $a_n(R)$ and $da_n(R)/dR$ enable the first eleven terms in the series formulae (42) and (43) for the field components h'_r , h'_θ to be computed for any point (r, θ) . Let S_n denote the sum of the first n terms in either case. It is found that as n increases from 1 to 11, the sums form an irregularly oscillating sequence; the convergence is slow for values of r near $k_0 a$, especially for small values of θ . Thus, for example, for $r = k_0 a$, $\theta = 0$, we have $h'_\theta = 0$ and

$$k_0^2 h'_r = \sum_{n=0}^{\infty} (2n+1)(2n+2)a_{2n+1}(k_0). \quad (47)$$

Table 2

The effects of Cesàro summation on the convergence of the series (48)

n	s_n	$c_n^{(1)}$	$c_n^{(2)}$
1	481	481	481
2	1259	870	740
3	1000	913	827
4	791	883	849
5	1239	954	884
6	797	928	897
7	1075	949	910
8	1001	955	920
9	925	952	926
10	791	936	928
11	678	912	925

The slow convergence is a consequence of the factor $(2n + 1)(2n + 2)$. Table 2 shows in the first column the sequence of partial sums

$$s_n = \sum_{s=0}^n (2s + 1)(2s + 2)a_{2s+1}(6) \tag{48}$$

for model I, calculated from our computed values.

The convergence of this type of series is greatly improved by the use of a process devised by Cesàro (1890). For the appropriate formulae see Bromwich (1908) Sections 122–128. If $\{s_n\}$ for $n = 0, 1, 2, \dots$ denotes the sequence of partial sums we define $S_n^{(0)} = s_n$,

$$S_n^{(m)} = S_0^{(m-1)} + S_1^{(m-1)} + \dots + S_n^{(m-1)} \tag{49}$$

and

$$c_n^{(m)} = S_n^{(m)} / \binom{n+m}{m}. \tag{50}$$

The Cesàro sum of degree m is then defined to be $c_m = \lim_{n \rightarrow \infty} \{c_n^{(m)}\}$, provided that this limit exists. If the original series is convergent, Cesàro’s mean value theorem states that its sum is c_m . Table 2 shows in the second and third columns the first and second Cesàro sums of the series shown in the first column. The reduction of oscillation of the sequence of Cesàro partial sums is notable. Physical considerations suggest that the original series must eventually converge, and we estimate that by using only the first Cesàro summation process the error in this region of poor convergence will not exceed a few per cent, and is probably as small as one per cent, provided that all Legendre functions up to the 21st are included in the summation. Probably only the first seven terms (i.e. all Legendre functions up to and including the 13th) are needed if the second Cesàro sum process is used. In this work we have only used the first Cesàro sum with eleven terms included in the summation. It should be noted that the formula for the n th partial sum is then

$$c_n^{(1)} = \frac{s_0 + s_1 + \dots + s_n}{n}. \tag{51}$$

6. The magnetic field lines and intensity

1. For the same data as in Section 3, model I, together with $n_0E = 150$, following Akasofu & Chapman (1961). Fig. 1 shows by full lines the field lines $\psi' = \text{constant}$ of the ring current belt alone. One unit on the diagram corresponds to a change of 20 units in ψ' as given by equation (37). The isolines of current intensity are also shown by broken curves, in unspecified units. The outer part of the current is westward and the inner part eastward.

Fig. 2 shows the lines of constant field intensity of the ring current belt alone, i.e. the isolines of $\sqrt{(h_r'^2 + h_\theta'^2)}$ obtained from equations (43) and (44). Figs. 1 and 2 both show a nearly uniform magnetic field in the central region. The units are as in (43) and (44). The results, based on the eleven term series for A , may have an accuracy not higher than one or two per cent.

Fig. 3 shows by full lines the field lines of the combined field $\mathbf{h} + \mathbf{H}$ of the radiation belt and the geomagnetic dipole. The corresponding undisturbed \mathbf{H} field lines of the dipole are shown by broken curves. This shows how the hot plasma forces the magnetic field lines outwards, as indicated by Parker (1962). Thus a given

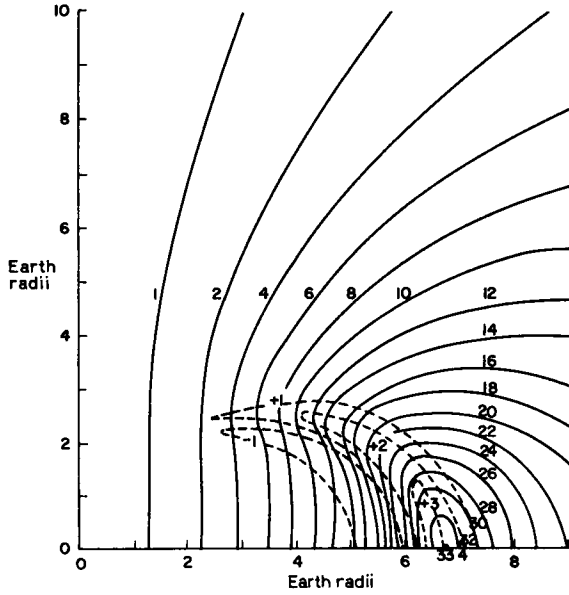


FIG. 1.

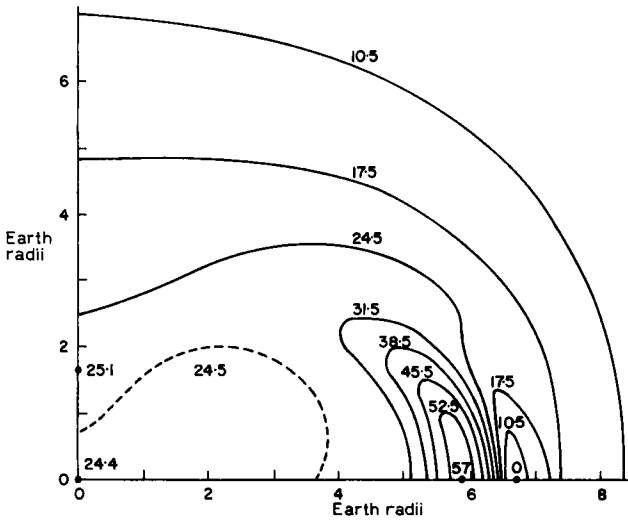


FIG. 2.

latitude on the Earth's surface may be magnetically connected by a growing ring current to regions of the magnetosphere more distant than normal.

II. For the same data as in Section 3, model II, together with $n_0E = 300$. Fig. 4 shows the field lines of the ring current belt alone (solid) together with the isolines of westward and eastward current intensity (broken). Fig. 5 shows the lines of constant field intensity for the ring current belt alone. Fig. 6 shows the field lines of the ring current belt combined with those of the geomagnetic dipole, and by broken curves the corresponding undisturbed dipole field lines. These three diagrams are similar to Figs. 1-3.

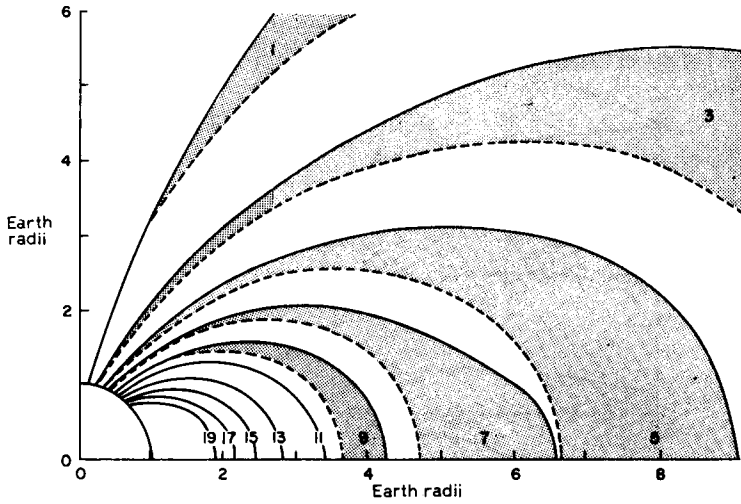


FIG. 3.

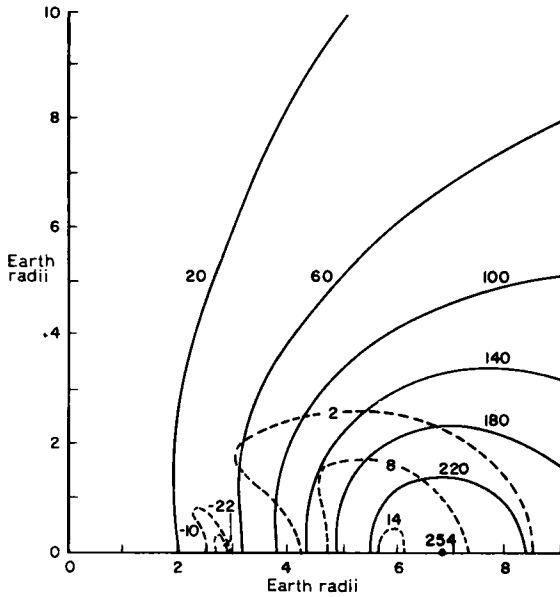


FIG. 4.

7. The magnetic *L* shells

Table 1 may be used to construct a table of values of the stream function $-0.32 \sin^2\theta/R + \psi$, ($= \psi$ for the total magnetic field), along any curve \mathcal{C} . As the field lines are the family of curves $\psi = \text{constant}$ this offers the possibility of investigating accurately the topography of the magnetic field. For example, taking \mathcal{C} in turn to be a meridian line on the Earth's surface and a radial line in the equatorial plane, we may relate the magnetic *L* shells (McIlwain 1961) to their latitudes where they intersect the surface of the Earth. This has been done for models I and II of Section 6. Fig. 7 shows the latitudinal displacement $\Delta\theta$, towards

the equator, due either ring current, of the points where a given L shell intersects the surface of the Earth.

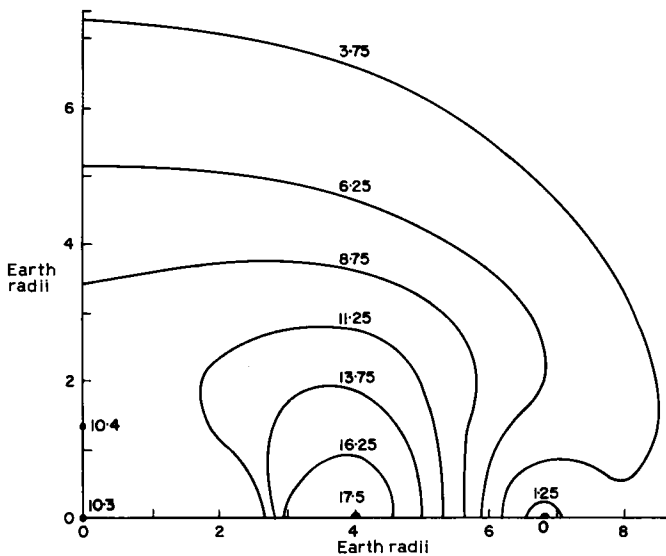


FIG. 5.

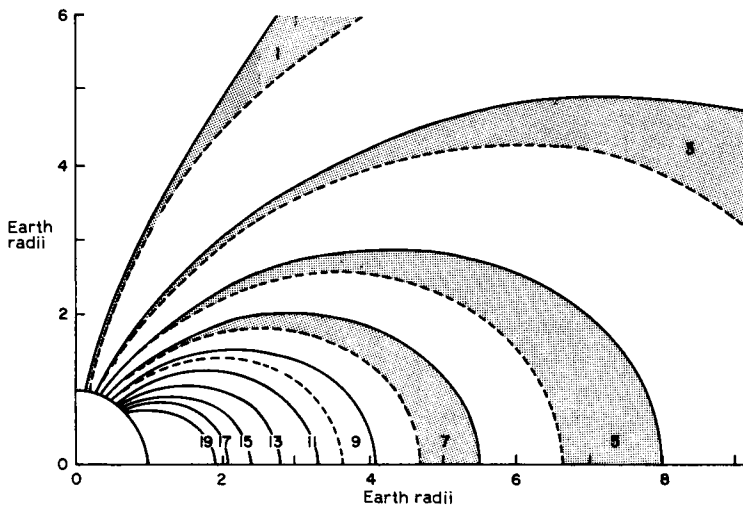


FIG. 6.

8. The distribution of magnetic energy in the various harmonics

From (43) and (44), the self magnetic energy is

$$W = 1.583 \times 10^{-14} a^3 (n_0 E)^2 \sum_{n=1}^{\infty} W_n \tag{52}$$

where if n is even $W_n = 0$, and if n is odd,

$$W_n = \frac{n(n+1)}{2(2n+1)} \int_0^{\infty} \left\{ \frac{n(n+1)a_n^2}{R^2} + \left(\frac{da_n}{dR} \right)^2 \right\} dR. \tag{53}$$

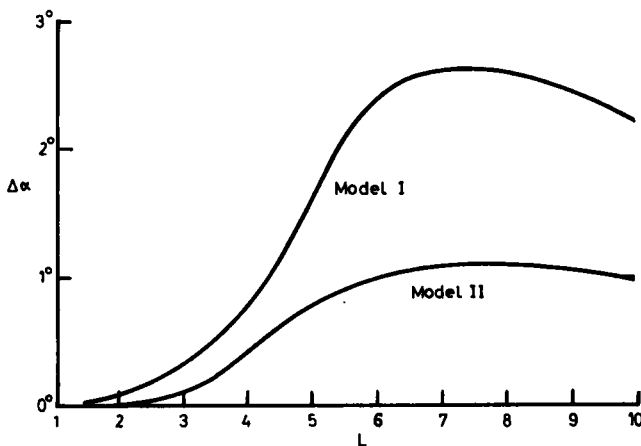


FIG. 7.

Using equation (41) this becomes

$$W_n = \frac{n(n+1)}{2(2n+1)} \left[(n+1)c_n^2 + \frac{nd_n^2}{10^{2n+1}} + \int_1^{10} \left\{ \frac{n(n+1)a_n^2}{R^2} + \left(\frac{da_n}{dR} \right)^2 \right\} dR \right]. \quad (54)$$

This has been evaluated for models I and II of Section 3 for all available harmonics. The results are shown in Table 3. Taking $a = 6370$ km and distinguishing the different cases by subscripts I and II gives

Model I, $W_I = 2.35 \times 10^{17} (n_0 E)_I^2 = 5.3 \times 10^{21}$ erg;

Model II, $W_{II} = 3.19 \times 10^{16} (n_0 E)_{II}^2 = 2.9 \times 10^{21}$ erg.

Chapman (1964) has recently discussed the change of magnetic field energy in the space around the Earth (and down to the depth below which Earth currents shield the interior from the changing outer fields), for different electric current

Table 3

The magnetic energies W_n of the various harmonics, together with $\sum_{n=1}^{n=21} W_n$

n	W_n (model I)	W_n (model II)
1	4.420×10^4	6.521×10^3
3	8.005×10^3	1.042×10^3
5	2.579×10^3	1.934×10^2
7	1.172×10^3	3.140×10
9	6.208×10^2	4.797
11	3.517×10^2	7.827×10^{-1}
13	2.069×10^2	1.381×10^{-1}
15	1.248×10^2	2.819×10^{-2}
17	7.668×10	8.489×10^{-3}
19	4.786×10	3.820×10^{-3}
21	3.027×10	2.085×10^{-3}
$\sum_{n=1}^{n=21} W_n$	5.742×10^4	7.793×10^3

distributions outside the Earth. For this purpose he used simple models in which the distributions were represented by one or more *surface* distributions, over spheres or planes. In particular he represented model I by two spherical current sheets, one of radius $6.5a$ carrying westward current, the other of radius $5.5a$ carrying eastward current (the ratio of the westward to the eastward current being 2:15:1): he also included a third spherical current sheet of radius $7a/8$ inside the Earth, representing the Earth currents; but this can be ignored in such calculations when the outer current system is more than $3a$ from the Earth's centre. Adjusting the current intensities in his and our calculations so that both give a field change of 100γ at the Earth's centre, his estimate of the field energy (model I) is 2.6×10^{22} erg, which agrees well with our more exact result of 2.5×10^{22} erg.

For the field energy of model II our result (adjusted to give a field change of 100γ at the Earth's centre) is 1.9×10^{22} erg, less different from the former than the large difference between the two model ring currents might lead one to expect.

For a given ring current field h_0 at the Earth's centre, the kinetic energy of the belt is independent of the distribution of particle density (Parker 1957); it is proportional to h_0 , by a factor which depends on the pitch angle distribution (Akasofu & Chapman 1961). For $\alpha = -0.5$ (model I) and $\alpha = 2$ (model II) the kinetic energies for $h_0 = 100\gamma$ are respectively 3.8×10^{22} erg and 5.6×10^{22} erg. Note that the field energy is proportional to h_0^2 ; also that at the Earth's surface the field dH caused by a changing ring current includes a part due to induced Earth currents, so that the ring current contribution h_0 may be only from a half to two thirds of dH .

Acknowledgments

One of us (P.C.K.) is very grateful to the High Altitude Observatory, Boulder, Colorado and the Geophysical Institute, College, Alaska, where much of this work was carried out. The work was partly supported by the United States Air Force Cambridge Research Center, through the European Office of Aerospace Research (OAR) under contract number AF EOAR 64-74.

References

- Akasofu, S.-I., 1963. *J. geophys. Res.*, **68**, 4437.
 Akasofu, S.-I., Cain, J. C. & Chapman, S., 1961. *J. geophys. Res.*, **66**, 4013.
 Akasofu, S.-I., Cain, J. C. & Chapman, S., 1962. *J. geophys. Res.*, **67**, 2645.
 Akasofu, S.-I. & Chapman, S., 1961. *J. geophys. Res.*, **66**, 1321.
 Bromwich, T. J. I'A., 1908. *An Introduction to Infinite Series*. Macmillan.
 Cesàro, E., 1890. *Bull. Sci. math.*, (2), **14**, 114.
 Chapman, S., 1964. *Geophys. J. R. astr. Soc.*, **8**, 514.
 Chapman, S. & Bartels, J., 1940. *Geomagnetism*. Oxford.
 Gauss, C. F., 1838. *Resultate Magn. Verein*; reprinted in *Werke*, **5**, 121.
 Kunz, K. S., 1957. *Numerical Analysis*. McGraw-Hill.
 McIlwain, C., 1961. *J. geophys. Res.*, **66**, 3681.
 Parker, E. N., 1957. *Phys. Rev.*, **107**, 924.
 Parker, E. N., 1962. *Space Sci. Rev.*, **1**, 62.
 Ralston, A. & Wilf, H. S., 1960. *Mathematical Methods for Digital Computers*. Wiley.
 Schuster, A., 1889. *Phil. Trans. R. Soc.*, A, **180**, 467.
 Smythe, W. R., 1950. *Static and Dynamic Electricity*. McGraw-Hill.